

RESEARCH ARTICLE

Optical and Temperature-Dependent Electrical Properties of $\text{Ge}_{1-x}\text{Pb}_x\text{O}_y$ Thin Films for Microbolometer Applications

ESAM S. BAHADRA¹, NAGEEB AL-KHALLI^{2,3}, MAHMOUD HEZAM^{3,4},
MOHAMMAD ALDURAIBI^{3,5}, NACER DEBBAR¹, AND MOHAMED ABDEL-RAHMAN²

¹College of Engineering, Electrical Engineering Department, King Saud University, Riyadh 11421, Saudi Arabia

²KACST-TIC in Radio Frequency and Photonics for the e-Society (RFTONICS), King Saud University, Riyadh 11421, Saudi Arabia

³King Abdullah Institute for Nanotechnology (KAIN), King Saud University, Riyadh 11451, Saudi Arabia

⁴College of Science, Physics Department, Imam Mohammad Ibn Saud Islamic University (IMSIU), Riyadh 13318, Saudi Arabia

⁵College of Science, Physics and Astronomy Department, King Saud University, Riyadh 11451, Saudi Arabia

Corresponding author: Mohammad Alduraibi (malduraibi@ksu.edu.sa)

This work was supported by the Deputyship for Research and Innovation, Ministry of Education, Saudi Arabia, under Project IFKSUOR3-372-1.

ABSTRACT In this study, an experimental investigation was conducted to explore $\text{Ge}_{1-x}\text{Pb}_x\text{O}_y$ as a candidate material for temperature-sensing layers in uncooled microbolometers. RF and DC sputtering techniques were used to deposit $\text{Ge}_{1-x}\text{Pb}_x\text{O}_y$ thin films with various oxygen concentrations on silicon substrates at room temperature. The composition of the samples was experimentally analyzed using energy dispersive X-ray spectroscopy (EDX) that showed various oxygen concentrations. Atomic force microscopy (AFM) analysis showed excellent average surface roughness ranging from 0.6995 to 0.8660 nm. Increasing the concentration of oxygen up to 31% improved the thermoelectric and optical characteristics of the prepared $\text{Ge}_{1-x}\text{Pb}_x\text{O}_y$ thin films. The highest temperature coefficient of resistance (TCR) of the fabricated samples was $-3.85\%/K$ for the $\text{Ge}_{0.94}\text{Pb}_{0.06}\text{O}_{0.31}$ thin film. By using Essential McLeod software, optical simulation of the thin film samples was performed to assess the highest absorbance of the cavity microbolometer structure, which was 81.88% for the $\text{Ge}_{0.94}\text{Pb}_{0.06}\text{O}_{0.31}$ thin film.

INDEX TERMS Germanium-lead (GePb), microbolometer, temperature coefficient of resistance, sputter deposition.

I. INTRODUCTION

The microbolometer is an uncooled resistive thermal detector that is widely used in the scientific field, defense, and industrial applications [1], [2], [3]. In general, a microbolometer requires thermal sensing materials with a high temperature coefficient of resistance (TCR) [4–7] and a relatively high infrared (IR) absorption, above 80%, in the $-12\ \mu\text{m}$ band for effective IR detection [8]. Vanadium oxide (VO_x) is commonly used as a sensing layer of microbolometers due to its high TCR of approximately $2\text{--}4\%/K$ [9], [10], [11]. Recently, many research groups have deeply addressed the use of silicon and germanium derivative compounds

as sensing layers for microbolometers. These compounds possess unique features that are beneficial for IR detectors, such as high TCRs and compatibility with silicon CMOS technology [12], [13], [14]. TCRs have been reported for some of these compounds, e.g., silicon-germanium (a-SiGe, poly-SiGe, and a- $\text{Ge}_x\text{Si}_{1-x}\text{O}_y$) showed TCR values from 2 to $8\%/K$ [10]; amorphous germanium tin alloy (a- $\text{Ge}_{1-x}\text{Sn}_x$) showed TCR values up to $3.96\%/K$ [15]; and amorphous silicon tin alloy (a- $\text{Si}_{1-x}\text{Sn}_x$) showed TCR values in the range from 1.72 to $3.25\%/K$ [16].

In this work, a novel thermal sensing material based on group IV semiconductors alloys for uncooled microbolometers is presented. The proposed sensor consists of thin films of $\text{Ge}_{1-x}\text{Pb}_x\text{O}_y$, which are inherently CMOS compatible. These thin films were synthesized by DC and RF sputtering

The associate editor coordinating the review of this manuscript and approving it for publication was Chaitanya U Kshirsagar.

in Ar and Ar:O₂ environments. Atomic force microscopy (AFM) and energy dispersive X-ray spectroscopy (EDX) were used to analyze the morphological and compositional properties of the prepared $\text{Ge}_{1-x}\text{Pb}_x\text{O}_y$ thin films. Moreover, ellipsometry was used to obtain the infrared optical constants n and k of the deposited films. Thin film optical simulations were performed to estimate the absorptance of the thin films in a microbolometer cavity configuration. Sheet resistance versus temperature measurements were performed and analyzed to predict the TCR and other electrical properties of the $\text{Ge}_{1-x}\text{Pb}_x\text{O}_y$ films.

II. EXPERIMENTAL STUDY

A. SAMPLE PREPARATION

$\text{Ge}_{1-x}\text{Pb}_x\text{O}_y$ thin films were fabricated by co-sputtering process using a 99.999% pure Ge target and a 99.99% pure Pb target in Ar and Ar:O₂ environments on SiO₂(300 nm)/Si substrates. All samples were deposited at room temperature using AJA International sputter coater at a chamber base pressure of 2×10^{-6} Torr and under an Ar or Ar:O₂ plasma pressure of 5 mTorr. To obtain thin films with different oxygen concentrations, the oxygen flow was set with different rates [0, 0.8, 1, and 1.2 sccm]. The RF power of the Ge target and DC power of the Pb target were held at 280 W and 10 W, respectively, during the deposition process.

The deposition time for each sample was adjusted to keep the grown thin films thickness around 200 nm, which was confirmed by using Veeco Dektak 150 surface profiler.

B. CHARACTERIZATION METHODS

The local elemental information of the materials was obtained by using an EDX silicon drift detector (Oxford INCA) attached to a JEOL 7600F FE-SEM. To perform accurate compositional analysis limited to the top $\text{Ge}_{1-x}\text{Pb}_x\text{O}_y$ thin film, EDX analysis was carried out using a low-energy electron beam with an acceleration voltage of 4 kV only. The surface roughness and grain size of the thin films were evaluated using a Veeco Multimode V atomic force microscope in tapping mode. The analysis was conducted on all samples to investigate the surface morphology of the prepared thin films.

Ellipsometric measurements of $\text{Ge}_{1-x}\text{Pb}_x\text{O}_y$ thin films were performed using a SENDIRA infrared ellipsometer in the wavelength range of 1.5 to 20 μm . Ellipsometric parameters ψ and Δ were recorded at 70°. The Drude-Lorentz oscillator model with eight Lorentz oscillators was used to fit the experimentally acquired ψ and Δ parameters in SpectraRay 3 software to extract the optical constants of the $\text{Ge}_{1-x}\text{Pb}_x\text{O}_y$ thin films [17], [18].

The operation of a microbolometer is based on the absorption of incident IR radiation by the thermal sensing layer. Therefore, a change in temperature causes a change in its electrical resistance [19]. Thermal characterization was

performed by measuring the temperature-dependent resistive behavior of all samples, and Jandel's four-point probe was used in conjunction with a temperature-controlled hot plate. The sheet resistance of the thin films was measured by using a four-point probe while varying the temperature from 20 to 70°C in 2°C steps. Then, the electrical parameters of $\text{Ge}_{1-x}\text{Pb}_x\text{O}_y$ thin film samples were calculated and extracted.

C. SIMULATION OF THE MICROBOLOMETER MULTILAYER DESIGN

The Essential McLeod thin film package is a comprehensive tool for designing and analyzing optical thin film multilayer structures [20]. Simulations were carried out within the LWIR spectral range from 8 to 12 μm by using $\text{Ge}_{0.94}\text{Pb}_{0.06}\text{O}_{0.06}$, $\text{Ge}_{0.94}\text{Pb}_{0.06}\text{O}_{0.22}$, $\text{Ge}_{0.94}\text{Pb}_{0.06}\text{O}_{0.27}$, and $\text{Ge}_{0.94}\text{Pb}_{0.06}\text{O}_{0.31}$ thin films as the thermal sensing layer, the atomic ratios were obtained from EDX results, as will be discussed in the following section. In the simulation, the cavity comprising absorbing layers and an air gap was considered as thin film multilayers stacked together to form cascaded Fabry-Perot optical cavities, each with different thicknesses and complex refractive index.

III. RESULTS AND DISCUSSION

A. COMPOSITIONAL AND MORPHOLOGICAL ANALYSIS

Fig. 1 shows that with the low-energy beam, acceleration voltage of 4 kV, the Si peak at 1.74 keV was completely absent. Hence, the oxygen signal was assumed to come from the deposited film and not from the SiO₂ underlayer. Since Ge and Pb target conditions were fixed for all samples and only the oxygen flow rate was changed during the deposition, the samples were expected to exhibit the formula $\text{Ge}_{1-x}\text{Pb}_x\text{O}_y$ with the same x for all samples and different y . This was confirmed by the EDX quantitative analysis; the Pb/(Pb+Ge) ratio was almost the same for all samples (~ 0.06). Oxygen was present in all samples, even the sample with “zero” inserted oxygen. Therefore, the contribution of post growth oxidation cannot be ignored, and without intentional oxygen exposure, the Pb:O ratio is 1:1. The atomic percentage of oxygen increases with increasing inserted reactive oxygen until a Pb:O ratio of 1:5.2 is reached at the highest oxygen concentration. Accordingly, the formulas for the four alloy samples may be written as $\text{Ge}_{0.94}\text{Pb}_{0.06}\text{O}_{0.06}$, $\text{Ge}_{0.94}\text{Pb}_{0.06}\text{O}_{0.22}$, $\text{Ge}_{0.94}\text{Pb}_{0.06}\text{O}_{0.27}$, and $\text{Ge}_{0.94}\text{Pb}_{0.06}\text{O}_{0.31}$. All samples are partially oxidized semiconductor alloys. The atomic percentage (at. %) and weight percentage (wt. %) for the samples elements are presented in Table 1.

The surface roughness and grain size of the thin films were analyzed by AFM, as shown in Fig. 2. The roughness values show no trend. However, they lie in a narrow range of 0.7-0.9 nm for average roughness. The $\text{Ge}_{0.94}\text{Pb}_{0.06}\text{O}_{0.06}$, $\text{Ge}_{0.94}\text{Pb}_{0.06}\text{O}_{0.22}$, $\text{Ge}_{0.94}\text{Pb}_{0.06}\text{O}_{0.27}$, and $\text{Ge}_{0.94}\text{Pb}_{0.06}\text{O}_{0.31}$ films have rms surface roughness values of 0.8994 nm,

TABLE 1. Atomic Percentage (at.%) and weight percentage (wt.%) of the samples elements.

Element	Sample 0		Sample 0.8		Sample 1.0		Sample 1.2	
	At. %	Wt. %	At. %	Wt. %	At. %	Wt. %	At. %	Wt. %
Ge L	87.07±0.97	81.58±1.41	76.95±2.51	80.94±1.00	72.65±2.96	79.00±1.84	70.65±0.78	78.86±1.03
Pb M	6.38±0.54	17.07±1.34	4.95±0.01	14.85±0.34	5.02±0.52	15.61±1.50	4.73±0.36	15.09±1.05
O K	6.55±0.50	1.35±0.10	18.12±2.50	4.21±0.66	22.41±2.95	5.39±0.83	24.62±0.71	6.06±0.22

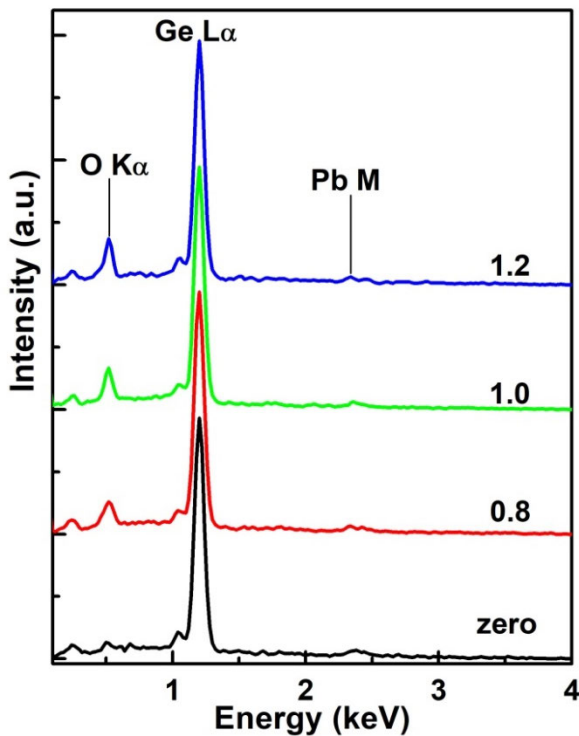


FIGURE 1. EDX spectra of the $\text{Ge}_{1-x}\text{Pb}_x\text{O}_y$ films grown at different oxygen concentrations, shows the intensity with respect to the energy for all compositions of the proposed materials.

1.1710 nm, 0.9466 nm, and 1.1050 nm, respectively. In general, the films have excellent surface morphology with very low roughness values.

B. ELLIPSOMETRY ANALYSIS

Ellipsometry was used to extract the optical properties of the proposed materials. The extracted refractive index n and extinction coefficient k of $\text{Ge}_{1-x}\text{Pb}_x\text{O}_y$ thin films were analyzed by spectroscopic ellipsometry in the wavelength range of 1.5 to 20 μm , as shown in Fig. 3. The refractive index n over the wavelength range decreases with increasing oxide content in the samples. The extinction coefficient k of all samples except for $\text{Ge}_{0.94}\text{Pb}_{0.06}\text{O}_{0.31}$ decreases in the wavelength range from 2 to 5 μm , and then, the extinction coefficient k increases for higher wavelengths up to 20 μm .

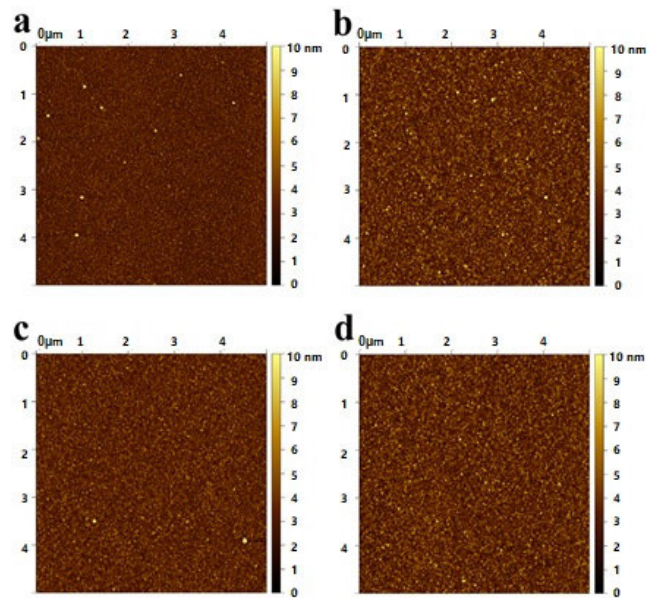


FIGURE 2. 2D AFM images of the prepared films with four different oxide percentages showing the (a) $\text{Ge}_{0.94}\text{Pb}_{0.06}\text{O}_{0.06}$, (b) $\text{Ge}_{0.94}\text{Pb}_{0.06}\text{O}_{0.22}$, (c) $\text{Ge}_{0.94}\text{Pb}_{0.06}\text{O}_{0.27}$ and (d) $\text{Ge}_{0.94}\text{Pb}_{0.06}\text{O}_0$ films.

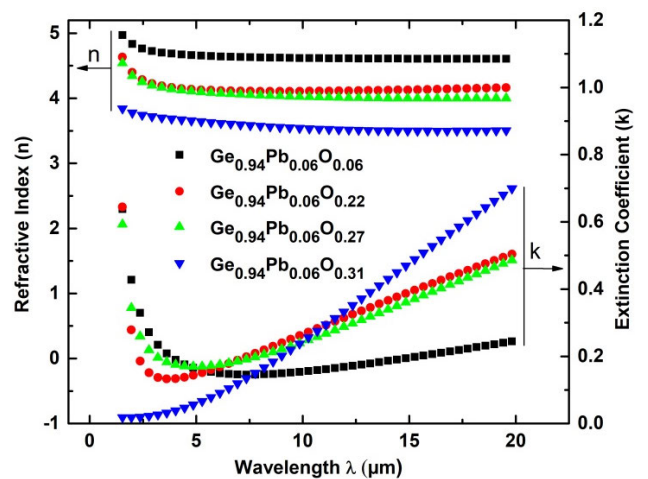


FIGURE 3. Refractive index (n) and extinction coefficient (k) as a function of wavelength for the four different $\text{Ge}_{1-x}\text{Pb}_x\text{O}_y$ films.

This increase in absorption was found to be associated with the increase in the oxygen content in the $\text{Ge}_{1-x}\text{Pb}_x\text{O}_y$ thin film.

C. OPTICAL SIMULATION

Fig. 4 shows the main structure layers of the proposed design, which was simulated in the Essential Macleod (EM) simulator environment. The main cavity microbolometer structure has the traditionally used materials adapted with the proposed novel material in this study, which is utilized as the active layer in the cavity microbolometer design. The obtained optical properties were employed in the EM simulator to analyze the cavity microbolometer structure. Because the microbolometer operates in the longwave infrared range, the analysis was performed to extract the absorptance of the microbolometer as a function of the long wavelength in the range from 8 to 12 μm. Fig. 5 illustrates that an increase in the oxide concentration in the Ge_{1-x}Pb_xO_y thin film enhances the absorptance of infrared radiation in the microbolometer cavity. The absorptance reaches a maximum of 81.88% for Ge_{0.94}Pb_{0.06}O_{0.31} at a wavelength of 12 μm.

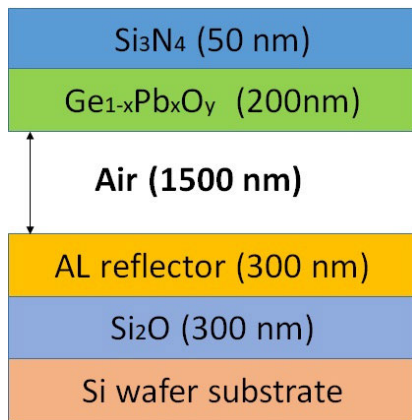


FIGURE 4. The main structure layers of the proposed design are simulated in the EM simulator.

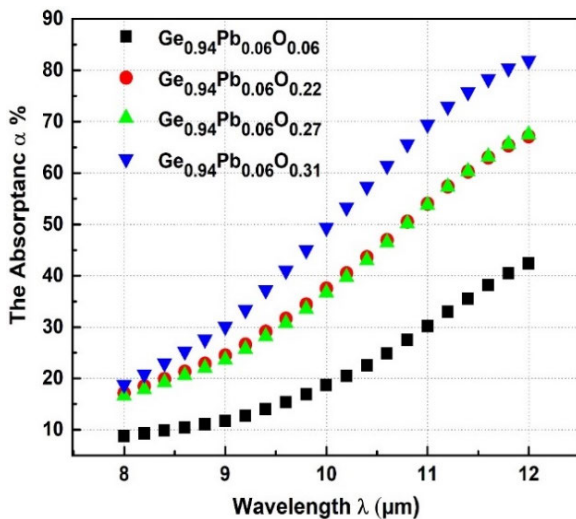


FIGURE 5. Simulation results of the absorptance vs. wavelength analysis of all proposed thin films.

D. ELECTRICAL CHARACTERIZATION

Jandel’s four-point probe and a temperature-controlled hot plate were used to measure the sheet resistance R_S of the prepared thin films at the same time when varying the temperature T from 20 to 70°C in 2°C steps. Fig. 6 shows the resistivity versus temperature curves for all synthesized Ge_{1-x}Pb_xO_y thin film samples. As seen from the obtained results in Fig. 6, Ge_{0.94}Pb_{0.06}O_{0.31} shows a maximum value of 153.6 Ω.cm compared with the other three samples.

The obtained results were adequately fitted using an exponential decay function, indicating semiconducting behavior of the grown Ge_{1-x}Pb_xO_y thin films, which followed the known Arrhenius relationship, as in Equation (1) [21].

$$\rho(T) = \rho_o \exp\left(\frac{E_a}{kT}\right) \quad (1)$$

where ρ is resistivity, ρ_o is the resistivity prefactor, E_a is the activation energy and k is Boltzmann’s constant. The activation energy E_a can be graphically determined by taking the natural logarithm of the Arrhenius equation, which is expressed as a line of the form $y = a + bx$. The TCRs of the amorphous Ge_{1-x}Pb_xO_y thin films were calculated using Equation (2) [21].

$$|TCR| = \left| \frac{1}{\rho} \frac{d\rho}{dT} \right| = \frac{E_a}{kT^2} \quad (2)$$

The values of the oxygen O₂%, R_S , ρ ($R_S \times$ film thickness), ρ_o , E_a , and TCR at room temperature for the fabricated thin films are summarized in Table 2. In general, the oxidation of Ge_{1-x}Pb_xO_y contributes to a decrease in the carrier mobility, so the sheet resistance, resistivity, and TCR of these samples increase. Furthermore, these Ge_{1-x}Pb_xO_y

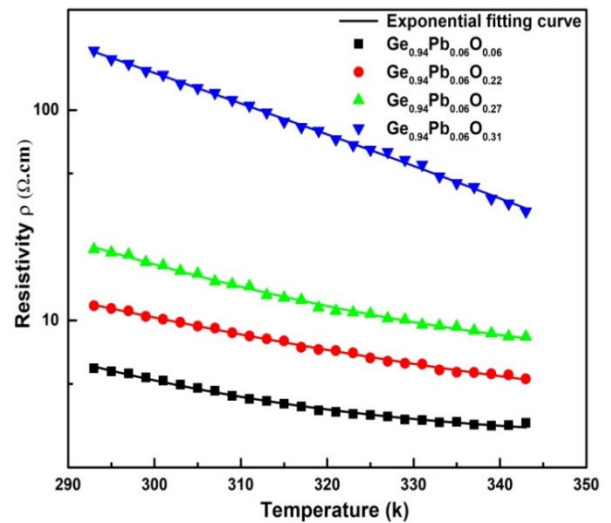


FIGURE 6. Resistivity versus temperature for the different Ge_{1-x}Pb_xO_y thin film samples.

TABLE 2. Summary of the electrical parameters of Ge_{1-x}Pb_xO_y thin film samples.

Samples	O ₂ %	R _S (MΩ/sq.)	ρ (Ω·cm)	ρ _o (mΩ·cm)	E _a (eV)	[TCR] %/K
Ge _{0.94} Pb _{0.06} O _{0.06}	6	0.268	5.36	64.2051	0.114	1.48
Ge _{0.94} Pb _{0.06} O _{0.22}	22	0.523	10.46	42.2635	0.142	1.84
Ge _{0.94} Pb _{0.06} O _{0.27}	27	0.946	18.92	22.0780	0.174	2.25
Ge _{0.94} Pb _{0.06} O _{0.31}	31	7.680	153.60	1.5140	0.297	3.85

films show high TCR values close to that of VO_x material which is currently used in the fabrication of uncooled microbolometers.

IV. CONCLUSION

In this work, amorphous Ge_{1-x}Pb_xO_y is introduced as a thermal sensing material in microbolometers. The sputter-deposited Ge_{1-x}Pb_xO_y was fabricated and examined to validate its use as a thermal sensing material in microbolometers. RF and DC sputtering deposition techniques with Ge and Pb targets in Ar and Ar:O₂ atmospheres were simultaneously used to produce room-temperature grown Ge_{0.94}Pb_{0.06}O_{0.06}, Ge_{0.94}Pb_{0.06}O_{0.22}, Ge_{0.94}Pb_{0.06}O_{0.27}, and Ge_{0.94}Pb_{0.06}O_{0.31} thin films. The experimental results show that the range of the TCR of the prepared samples is between -1.48 and -3.85%/K. In addition, the resistivity ranges between 5.36 and 153.6 Ω·cm. Moreover, the rms surface roughness of these samples was extracted from AFM measurements and found to range from 0.9 to 1.2 nm. Spectroscopic ellipsometry was used to extract the *n* and *k* of these materials experimentally. These extracted *n* and *k* values were used in a simulation study to find the absorptance of the thin films. The simulation results show that the absorptance increases with increasing oxide content of the samples. The absorptance reaches 81.88% for Ge_{0.94}Pb_{0.06}O_{0.31} at 12 μm. The Ge_{1-x}Pb_xO_y thin films have high TCR, acceptable resistivity, high absorptance, and good surface roughness. These properties make the proposed Ge_{1-x}Pb_xO_y materials practical for uncooled microbolometer technology.

ACKNOWLEDGMENT

The authors extend their appreciation to the Deputyship for Research and Innovation, Ministry of Education in Saudi Arabia for funding this research work through the project no. (IFKSUOR3-372-1).

REFERENCES

- [1] C.-N. Chen and J.-S. Shie, "Fabrication of a sensitive germanium microbolometer for tympanic thermometry," *Sensors Mater.*, vol. 11, no. 6, pp. 369–382, 1999.
- [2] Y.-Z. Deng, S.-F. Tang, H.-Y. Zeng, Z.-Y. Wu, and D.-K. Tung, "Experiments on temperature changes of microbolometer under blackbody radiation and predictions using thermal modeling by COMSOL multiphysics simulator," *Sensors*, vol. 18, no. 8, p. 2593, Aug. 2018.
- [3] E. Mottin, A. Bain, J.-L. Martin, J.-L. Ouvrier-Bufferet, S. Bisotto, J.-J. Yon, and J.-L. Tissot, "Uncooled amorphous silicon technology enhancement for 25-μm pixel pitch achievement," *Proc. SPIE*, vol. 4820, pp. 200–207, Jan. 2003.

- [4] M. Almasri, B. Xu, and J. Castracane, "Amorphous silicon two-color microbolometer for uncooled IR detection," *IEEE Sensors J.*, vol. 6, no. 2, pp. 293–300, Apr. 2006.
- [5] N. Chi-Anh, H.-J. Shin, K. Kim, Y.-H. Han, and S. Moon, "Characterization of uncooled bolometer with vanadium tungsten oxide infrared active layer," *Sens. Actuators A, Phys.*, vols. 123–124, pp. 87–91, Sep. 2005.
- [6] M. Almasri, M. Hai, M. Hesani, M. Cheng, Q. Jalal, A. J. Syllaios, and S. Ajmera, "Uncooled infrared microbolometers and silicon germanium oxide (Si_xGe_{1-x}O_y) infrared sensitive material for long wavelength detection," Dept. Elect. Eng. Comput. Sci., Univ. Missouri, Columbia, MO, USA, Tech. Rep. W911NF-09-1-0158, 2014.
- [7] G.-H. Koo, Y.-C. Jung, S.-H. Hahm, D.-G. Jung, and Y.-S. Lee, "Characteristic of nickel oxide microbolometer," *Proc. SPIE*, vol. 8704, Jun. 2013, Art. no. 87041P.
- [8] S. G. Choi, T.-J. Ha, B.-G. Yu, S. Shin, H. H. Cho, and H.-H. Park, "Application of mesoporous TiO₂ as a thermal isolation layer for infrared sensors," *Thin Solid Films*, vol. 516, nos. 2–4, pp. 212–215, Dec. 2007.
- [9] D. S. Tezcan, O. S. Akar, and T. Akin, "An uncooled microbolometer infrared detector in any standard CMOS technology," in *Proc. 10th Int. Conf. Solid-State Sensors Actuators*, Jun. 1999, pp. 610–613.
- [10] A. Voshell, N. Dhar, and M. M. Rana, "Materials for microbolometers: Vanadium oxide or silicon derivatives," *Proc. SPIE*, vol. 10209, Apr. 2017, Art. no. 102090M.
- [11] Y. O. Jin, A. Ozcelik, M. W. Horn, and T. N. Jackson, "Potential for reactive pulsed-DC magnetron sputtering of nanocomposite VO_x microbolometer thin films," *J. Vac. Sci. Technol. A, Vac., Surf., Films*, vol. 32, no. 6, Nov. 2014, Art. no. 061501.
- [12] M. Moreno, A. Kosarev, A. Torres, and R. Ambrosio, "Microbolometers fabricated with surface micromachining with a-Si-Ge:H THERMO-sensing films," *Int. J. High Speed Electron. Syst.*, vol. 18, no. 4, pp. 1045–1054, Dec. 2008.
- [13] C. Calaza, N. Viarani, G. Pedretti, M. Gottardi, A. Simoni, V. Zanini, and M. Zen, "An uncooled infrared focal plane array for low-cost applications fabricated with standard CMOS technology," *Sens. Actuators A, Phys.*, vol. 132, no. 1, pp. 129–138, Nov. 2006.
- [14] F. Forsberg, A. C. Fischer, G. Stemme, N. Roxhed, F. Niklaus, P. Ericsson, and B. Samel, "High-performance infrared micro-bolometer arrays manufactured using very large scale heterogeneous integration," in *Proc. 16th Int. Conf. Opt. MEMS Nanophotonics*, Aug. 2011, pp. 9–10.
- [15] M. Abdel-Rahman, M. Alduraibi, M. Hezam, and B. Ilahi, "Sputter deposited GeSn alloy: A candidate material for temperature sensing layers in uncooled microbolometers," *Infr. Phys. Technol.*, vol. 97, pp. 376–380, Mar. 2019.
- [16] H. ElGhoniemy, M. R. Abdel-Rahman, M. Hezam, M. Alduraibi, N. Al-Khalli, and B. Ilahi, "Amorphous SiSn alloy: Another candidate material for temperature sensing layers in uncooled microbolometers," *Phys. Status Solidi (b)*, vol. 258, no. 11, Nov. 2021, Art. no. 2100103.
- [17] M. R. Abdel-Rahman, "Vanadium oxide thin films with high midwave & longwave infrared thermo-optic coefficients and high temperature coefficients of resistance," *Optik*, vol. 159, pp. 79–86, Apr. 2018.
- [18] M. F. Zia, M. Abdel-Rahman, M. Alduraibi, B. Ilahi, E. Awad, and S. Majzoub, "Electrical and infrared optical properties of vanadium oxide semiconducting thin-film thermometers," *J. Electron. Mater.*, vol. 46, no. 10, pp. 5978–5985, Oct. 2017.
- [19] M. Moreno, A. Torres, R. Ambrosio, and A. Kosarev, "Un-Cooled Microbolometers with Amorphous Germanium-Silicon (a-Ge_xSi_y:H) Thermo-Sensing Films. IntechOpen, 2012.
- [20] *Essential-Macleod Software Package*. Accessed: May 18, 2023. [Online]. Available: www.thinfilmcenter.com
- [21] R. A. Wood, "Chapter 3 monolithic silicon microbolometer arrays," in *Semiconductors and Semimetals*, vol. 47. Plymouth, MN, USA: Elsevier, 1997, pp. 43–121d.

ESAM S. BAHADRA was born in Ghayl Ba Wazir, Hadhramout, Yemen, in 1981. He received the B.S. degree in electronic and communication engineering from the University of Hadhramout, in 2006, and the M.S. degree in electrical engineering from King Saud University, Riyadh, Saudi Arabia, in 2016, where he is currently pursuing the Ph.D. degree in electronics engineering with the College of Engineering. His research interests include the characterization and fabrication of micro- or nano-structured surfaces of thin film and electronic devices, such as microbolometers, in addition to administrating and implementing solar cell systems while enhancing and consuming rationalizing energy.



ogy, KSU. His research interests include photodiodes and microbolometer design and fabrication.

MAHMOUD HEZAM received the B.Sc. and M.Sc. degrees in physics from the King Fahd University of Petroleum and Minerals (KFUPM), in 2004 and 2007, respectively, and the Ph.D. degree in physics from École Polytechnique Fédérale de Lausanne (EPFL), in 2017. He was a Researcher with the King Abdullah Institute for Nanotechnology (KAIN). He is currently with the Physics Department, Imam Mohammad Ibn Saud Islamic University (IMSIU), as an Assistant Professor. His research interests include semiconductor materials and devices for energy and other optoelectronic applications.

MOHAMMAD ALDURAIBI received the B.Sc. degree in physics from King Saud University, Saudi Arabia, in 2000, the M.Sc. degree in nanoscale science and technology from the University of Leeds, U.K., in 2006, and the Ph.D. degree in microelectronics and nanostructures from The University of Manchester, U.K., in 2010. He is currently an Associate Professor with the Department of Physics and Astronomy, King Saud University. His research interests include the growth and characterization of nanostructured semiconductor materials in addition to the fabrication and testing of a variety of advanced electronic and optoelectronic devices.



NACER DEBBAR received the DES degree in physics from the University of Constantine, Algeria, in 1982, and the M.S. degree in electrical science and the Ph.D. degree in electrical engineering from the University of Michigan, Ann Arbor, in 1984 and 1989, respectively. From 1990 to 1992, he conducted postdoctoral studies in the area of high-speed optoelectronic devices and optoelectronic integration with EPFL, Lausanne, Switzerland. For one year, he held a Visiting Postdoctoral position with Bilkent University, Ankara, Turkey. From 1993 to 1995, he was an Assistant Professor with the Physics Department, United Arab Emirates University. In 1995, he joined King Saud University, Saudi Arabia, as an Assistant Professor of electrical engineering, where he has been a Professor, since 2017. His research interests include modeling and simulation of semiconductor devices, especially GaAs-based and ZnO-based devices, and heterostructure.

MOHAMED ABDEL-RAHMAN received the Ph.D. degree in electrical engineering from the University of Central Florida (UCF), Orlando, FL, USA. He was a Professor with the Electrical Engineering Department, King Saud University, Riyadh, Saudi Arabia. He was previously associated with the Prince Sultan Advanced Technologies Research Institute (PSATRI), where he established and was the Director of the Electro-Optics Laboratory (EOL). He has published more than 50 international journal and conference papers. He is a holder of four U.S. patents. His research interests include microelectronics devices and sensors, electronics and optical materials, microfabrication, microlithography, infrared/millimeter wave detectors, and focal plane arrays. He is a winner of the Almarai/KACST Award for innovation, in 2015.

• • •